JOURNAL OF MATERIALS SCIENCE **34** (1999) 5407–5416

Influence of the particle size and phase type of zirconia on the fabrication and residual stress of zirconia/stainless-steel 304 functionally gradient material

Y. G. JUNG
Department of Ceramic Science and Engineering, Changwon National University, Korea
E-mail: jungyg@sarim.changwon.ac.kr

U. PAIK, S. C. CHOI
Department of Ceramic Engineering, Hanyang University, Seoul 133-791, Korea

Tetragonal zirconia polycrystal (TZP)/stainless steel 304 (SUS304)- and ZT [50 vol % monoclinic zirconia polycrystal (MZP) + 50 vol % TZP]/SUS304-functionally gradient material (FGM) were fabricated by pressureless sintering, and the sintering properties and residual stresses of this proposed FGM were compared with directly jointed material. The defects in the sintered specimens, such as warping, frustum formation, delamination, and cracking, which originated from the different shrinkage and sintering behavior of ceramic and metal, could be controlled by the adjustments in terms of the particle size and phase type of zirconia. The residual stresses induced on the ceramic and metal regions of FGM were characterized by the X-ray diffraction method, which were relaxed as the thickness and number of compositional gradient layers were increased. The residual stresses in TZP/SUS304-FGM show irregular patterns resulting from sintering defects and thermal expansion mismatch. In ZT/SUS304-FGM, compressive stress is induced on the ceramic regions by the volume expansion of MZP that resulted from the t $\rightarrow$ m ZrO_2 phase transformation on cooling. Also, compressive stress is induced on the metal regions by the constraint of warping and frustum formation that must be created to the metal direction caused by the difference of the coefficient of thermal expansions. As a consequence, it has been verified that the residual stresses generated on FGM are dominantly influenced by the thickness and number of compositional gradient layers, and the sintering defects and residual stresses can be controlled by the decrease of the difference of the shrinkage and sintering behavior of each component.

1. Introduction

The rapid progress of high technology, especially in energy and electronic applications, requires the development of advanced materials having not only a specific function but also superior properties such as thermal barrier, thermal shock resistance, anti-corrosion, and high reliability, which are possible for use under severe environments of extremely high temperature and applied thermal stress [1–4]. Because general composite materials cannot be expected to meet these requirements, nano-composites with nano-order dispersed phases and fine-composites have been proposed for various functions [5, 6]. Even though the thermal barrier coating and ceramic/metal joining techniques have been undertaken for the application of ultra-high-temperature materials [7–9], the ceramic/metal interface in these composites could be regarded as a major weakness in the materials themselves. At this interface, the sudden changes on the thermal properties often result in the thermal stress concentration, followed by catastrophic failure. Thus, there is a need to develop a functionally gradient material (FGM) having a compositional gradient from one surface of the material to the other [10–15]. In FGM, the composition of the dispersion phase is gradually and spatially varied, thus the properties/microstructure relationships have continuous characteristics. These features of FGM are expected to reduce or even eliminate residual stress as well as to control thermal barrier characteristics.

In this work, ceramic/metal–FGM with a combination of zirconia (tetragonal zirconia polycrystal (TZP) or ZT) and stainless steel 304 (SUS304) have been pressureless sintered and then investigated extensively to understand the various problems of the fabrication process and the application of FGM. The sintering process is thought to be one of the most viable routes for FGM, in which a wide range of composition and microstructure control can be allowed along with shape-forming

TABLE I Properties of starting materials

Properties / Materials	Melting point (°C)	Density (10^3 Kg/m^3)	Mean coefficient of thermal expansions (10^{-6}/°C)	Modulus of elasticity (GPa)	Poisson's ratio	Mean particle size (μm)	Specific surface (m^2/g)
TZP*	2719	6.05	9.6(20 ~ 400 °C) 11.8(20 ~ 1000 °C)	186(20 °C)	0.31	0.3	15.8
MZP**	2677	5.56	6.5(20 °C)	210(20 °C)	0.3	14	1 ~ 2
SUS304***	1400 ~ 1450	8.06	17.2(20 ~ 100 °C) 18.4(20 ~ 538 °C)	193(20 °C)	0.3	2 ~ 10	—

*3 mol % Y_2O_3-doped tetragonal zirconia polycrystal.
**Monoclinic zirconia polycrystal.
***Stainless steel 304.

capability [13–15]. The residual stresses induced on the ceramic and metal regions of FGM on cooling from sintering temperature were analyzed by the X-ray diffraction (XRD) method [16, 17], especially in the ceramic regions, and compared to results from the indentation method [18].

2. Experimental procedure

2.1. Starting materials and fabrication process

The starting materials were 3 mol % Y_2O_3-doped TZP (Tosoh Corp., Japan), which has an excellent thermal barrier property, anti-corrosion, and wear resistance, and powder mixture (ZT) of 50 vol % monoclinic zirconia polycrystal (MZP, Imperial Polychemicals Corp., USA, SC30) and 50 vol % TZP. The mixtures were used to control the different shrinkage and sintering behavior of ceramic and metal powders [14, 19, 20]. SUS304 (Nilaco Corp., Japan, 99.8%) was selected as a metal component, which has been applied to the anti-corrosion materials for anti-oxidation and strength at high temperature [21]. The properties of the starting materials are shown in Table I.

Two kinds of FGM, TZP/SUS304-FGM and ZT/SUS304-FGM, were fabricated by pressureless sintering, as shown in the experimental procedure of Fig. 1. After ball-milling for 12 h, the controlled particles of TZP (median size $\simeq$ 0.13 μm), MZP (median size $\simeq$ 4.12 μm), and SUS304 (median size $\simeq$ 5.02 μm), respectively, could be obtained. When metal composition was above 85 vol %, 0.5 wt % polyvinyl alcohol (PVA) was added to increase the formability of the green body. The prepared disc-type green bodies of each composition, which have 0.5 mm and 1 mm thickness and 10 mm diameter, were stacked in steel die with 5 vol %, 10 vol %, 50 vol % and 100 vol % compositional gradient, and then compacted at $\leq$50 MPa ($\leq$0.5 ton/mm^2). Deposited compacts were cold isostatic pressed (CIP) at 200 MPa and pressureless sintered for 2 h at 1350 °C in 1 atm Ar-atmosphere.

In general, FGM can be classified into three kinds according to the stacking methods of compositional gradient layer: (1) functionally gradient plate (FGP), which continuously changes the composition from ceramic to metal; (2) functionally gradient coating (FGC), which builds up the FGP on ceramic- or metal-monoliths; and (3) functionally gradient joint (FGJ), which builds up the FGP between ceramic- and metal-monoliths. Each of these three kinds of FGM was fabricated with

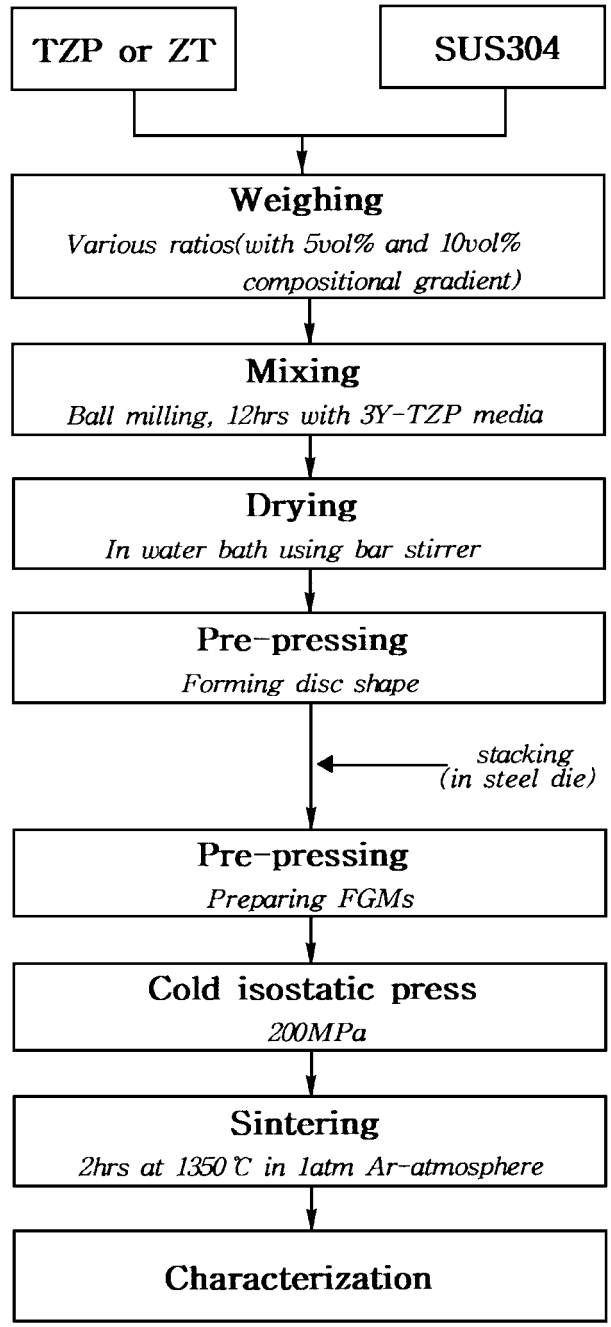

Figure 1 Schematic diagram of the experimental procedure.

TZP/SUS and ZT/SUS systems at the same conditions. The thickness of the ceramic- and metal-monoliths in FGC, FGJ, and directly jointed material (DJM) were about 5 ~ 6 mm. The sintering temperature and

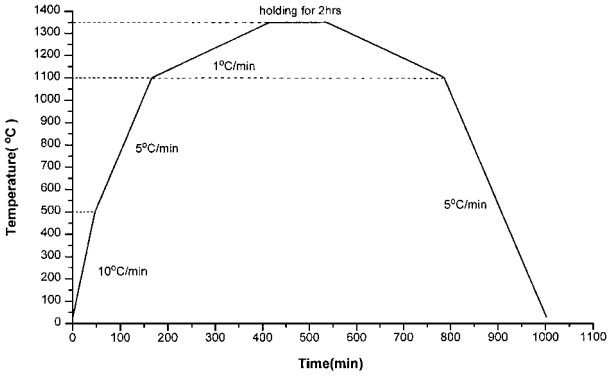

Figure 2 Sintering schedule of TZP/SUS304 and ZT/SUS304 systems to relax the residual stress and increase the sinterability of ceramic material.

time were constrained by the melting temperature of SUS304 (1400 ∼ 1450 °C) and the shrinkage rates of each component. Heating and cooling were performed to relax the residual stress and increase the sinterability of ceramics, as shown in Fig. 2.

2.2. Properties analysis

The variation and amount of sintering shrinkage in TZP/SUS304 and ZT/SUS304 systems were observed in the sintered bodies of each composition, which were sintered up to 1350 °C at an interval of 50 °C. The microstructure was observed with an optical microscope (Reichert Metaplan 2, Leica, Austria) and a stereoscope (Olympus, Japan). Residual stress states induced on the ceramic (TZP and ZT)-monolith and the ceramic regions of FGM were investigated with a Vickers hardness tester (Model DVKH-1, Japan). The residual stresses induced on the ceramic and metal regions of FGM were examined by using an X-ray stress analyzer (CN2905G3, Regaku, Japan) and compared with those of DJM. The determination of stress by XRD is based on the measurement of lattice strain, which can be obtained from the angular shift of the diffraction profile investigated [16, 17].

In the X-ray stress analysis, various methods have been proposed depending upon the incidence angle of the X-ray [16, 17, 22, 23]. The so-called $\sin^2\psi$ method [23] was used in this work to determine stress, which is calculated according to following equation:

$$\sigma_\phi = -\frac{E}{2(1+\nu)}\cot\theta\frac{\partial(2\theta)}{\partial\sin^2\psi}$$

A stress component σ_ϕ is given by the slope M of the least-mean-square line obtained from the plot of measured diffraction profiles 2θ as a function of $\sin^2\psi$. Considering specific diffraction plane, we obtain the X-ray elastic constant K as

$$\frac{E}{2(1+\nu)}\cot\theta = K$$

Therefore, the stress component σ_ϕ in the ϕ direction is expressed by

$$\sigma_\phi = KM$$

TABLE II X-ray elastic constants of ceramic and metal and XRD conditions for residual stress measurement

Material / Condition	ZrO_2(TZP)	SUS304
Characteristic X-ray	CrK_α	
Filter	Ni	
Tube voltage (kV)	30	
Tube current (mA)	35	
Measurement system	Ordinary goniometer	
Slit (mm)	1	
Diffraction plane	(3 3 1)	(2 2 0)
Diffraction angle (deg)	155.7	128.7
Fixed time	70	60
Young's modulus (Kgf/mm^2)	21 836	19 600
Poisson's ratio	0.31	0.28
Stress constant	−31.301	−64.13

According to the sign of the slope, negative and positive refer to tensile and compressive stress states, respectively. The incidence angle was selected as 0°, 10°, 20°, 30°, and 40° in this work. The X-ray elastic constants of ceramic and metal and the XRD conditions for the residual stress determination are given in Table II.

3. Results and discussion

3.1. Sintering characteristics and microstructure

The green layer compacts with the different mixing ratios of ceramic and metal were found to show the different shrinkage and sintering behavior. Differential sintering shrinkage causes the various flaws in the sintered specimens, such as warping, frustum formation, delamination, and cracking. To control these flaws, three parameters of the shrinkage behavior must be taken into account: (1) the shrinkage starting temperature; (2) the slope of the shrinkage curve versus temperature; and (3) the final net shrinkage [14]. At present, the size control of starting powders, adjustment of mixing conditions, pressure sintering (hot-pressing or hot isostatic pressing), and temperature gradient sintering have been proposed as the methods for manipulating these three parameters [24, 25].

In this work, the control of the shrinkage and sintering behavior in terms of the three parameters could be accomplished by the adjustments of the particle size and phase type of zirconia. From the results of the observed shrinkage behavior in TZP/SUS304 and ZT/SUS304, composites of each composition at each temperature, as shown in Figs 3 and 4, it is known that TZP/SUS304 composites have a wider range than ZT/SUS304 composites in the shrinkage curve, and the difference of the final net shrinkage is about 10% in TZP/SUS304 composites. These differences of the shrinkage have been thought to cause the sintering defects mentioned above. However, in ZT/SUS304 composites, troublesome effects of the sintering unbalance can be largely avoided by the relatively narrower shrinkage curve and smaller final net shrinkage than those of TZP/SUS304 composites and the volume expansions (3 ∼ 4%) on cooling caused by the t → m ZrO_2 phase transformation of MZP. Especially, the phase transformation has

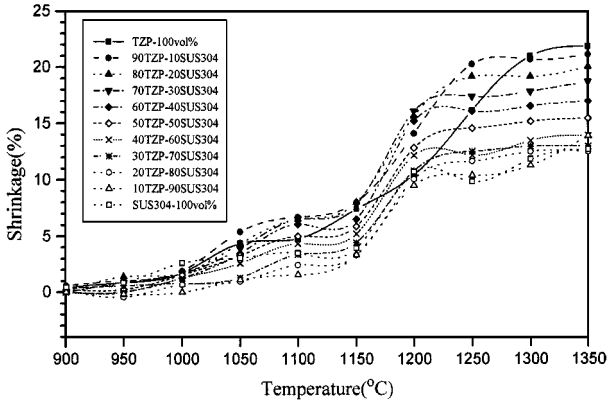

Figure 3 Effect of metal volume fractions and sintering temperature on sintering shrinkage in TZP/SUS304 composites.

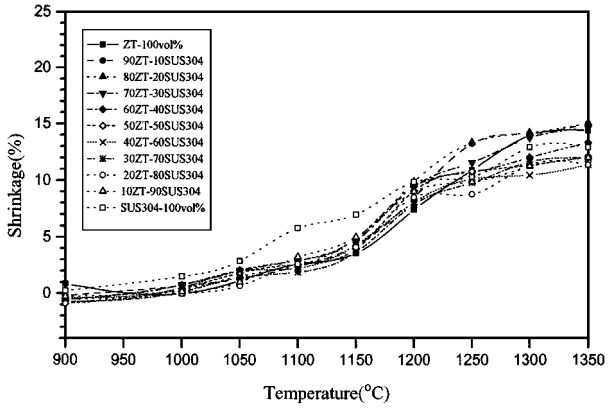

Figure 4 Effect of metal volume fractions and sintering temperature on sintering shrinkage in ZT/SUS304 composites. Adjustment of sintering shrinkage by controlling the particle size and phase type of zirconia.

been thought to counteract some of the effects of differential sintering shrinkage.

Figs 5–7 show the samples produced in TZP/SUS304 and ZT/SUS304 systems. In the case of DJM without an interlayer or with one interlayer (50 vol % ceramic/50 vol % metal) as shown in Fig. 5, radial cracks developed from the free surface and propagated to the center of the ceramic regions in both the TZP/SUS304 and ZT/SUS304 systems. It is thought that these cracks are due to the difference of the shrinkage and sintering behavior and the difference in the CTEs between ceramic and metal. Fig. 6a, c, and d show the warping observed in TZP/SUS304-FGP. In TZP/SUS304-FGM having the same interlayers (9 interlayers), the warping decreases but delamination occurs in the metal-rich (80 vol % metal) regions as the thickness of the interlayer is increased. It is believed that the sintering defects in TZP/SUS304-FGP, such as warping and delamination, occur as follows: The warping in the ceramic direction is due to the different shrinkage behavior of layers and the plastic deformation of the metal regions at elevated temperatures to relax thermal stress. The delamination in the metal-rich regions is due to the difference of the CTEs between ceramic and metal and the constraint of the ceramic material on cooling. Therefore, if the thickness and number of interlayers are increased, the difference of the shrinkage behavior and CTEs of layers will be decreased. As a result, the warping decreases and the delamination disappears, as shown in Fig. 6d. In the case of the thin thickness layer, because the effect of the shrinkage behavior is larger than that of the difference of the CTEs, severe warping occurs instead of delamination. On the other hand, the warping and cracking observed in TZP/SUS304-FGP do not occur in ZT/SUS304-FGP (frustum formation of Fig. 6e was made during polishing), which resulted from the similar shrinkage behavior (Fig. 4) and the volume expansion of MZP on cooling. Fig. 7 shows the surface photographs of TZP/SUS304-FGC, ZT/SUS304-FGC, and TZP/SUS304-FGJ. In TZP/SUS304-FGC, the delamination is created at the interface between the composite layer (90 vol % metal layer) and the metal-monolith. But in ZT/SUS304-FGC, which has the same interlayers but different thickness than TZP/SUS304-FGC, the sintering defects do not occur. In TZP/SUS304-FGJ, having 19 interlayers, the cracking in the ceramic regions and the metal-rich (80 ∼ 85 vol % metal) regions appears. It is thought to be the influence of the shrinkage and sintering behavior. Fig. 8 shows the cracks observed in TZP/SUS304-FGP. It is thought that these cracks are caused by the differential sintering shrinkage of starting materials (ceramic and metal) and the

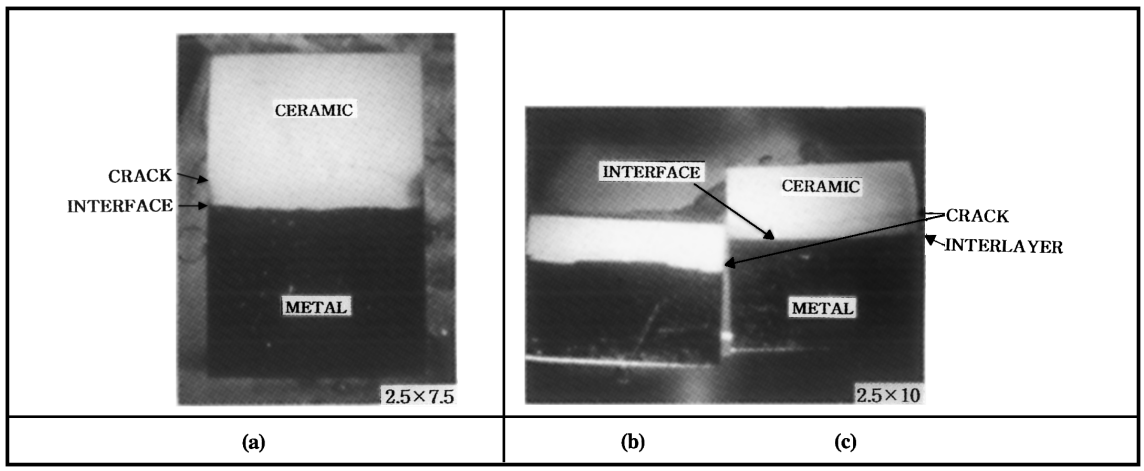

Figure 5 Photographs of sintering samples: (a) directly jointed TZP/SUS304; (b) TZP/interlayer/SUS304 having one interlayer (50 vol % TZP/50 vol % metal); and (c) ZT/interlayer/SUS304 having one interlayer (50 vol % ZT/50 vol % metal).

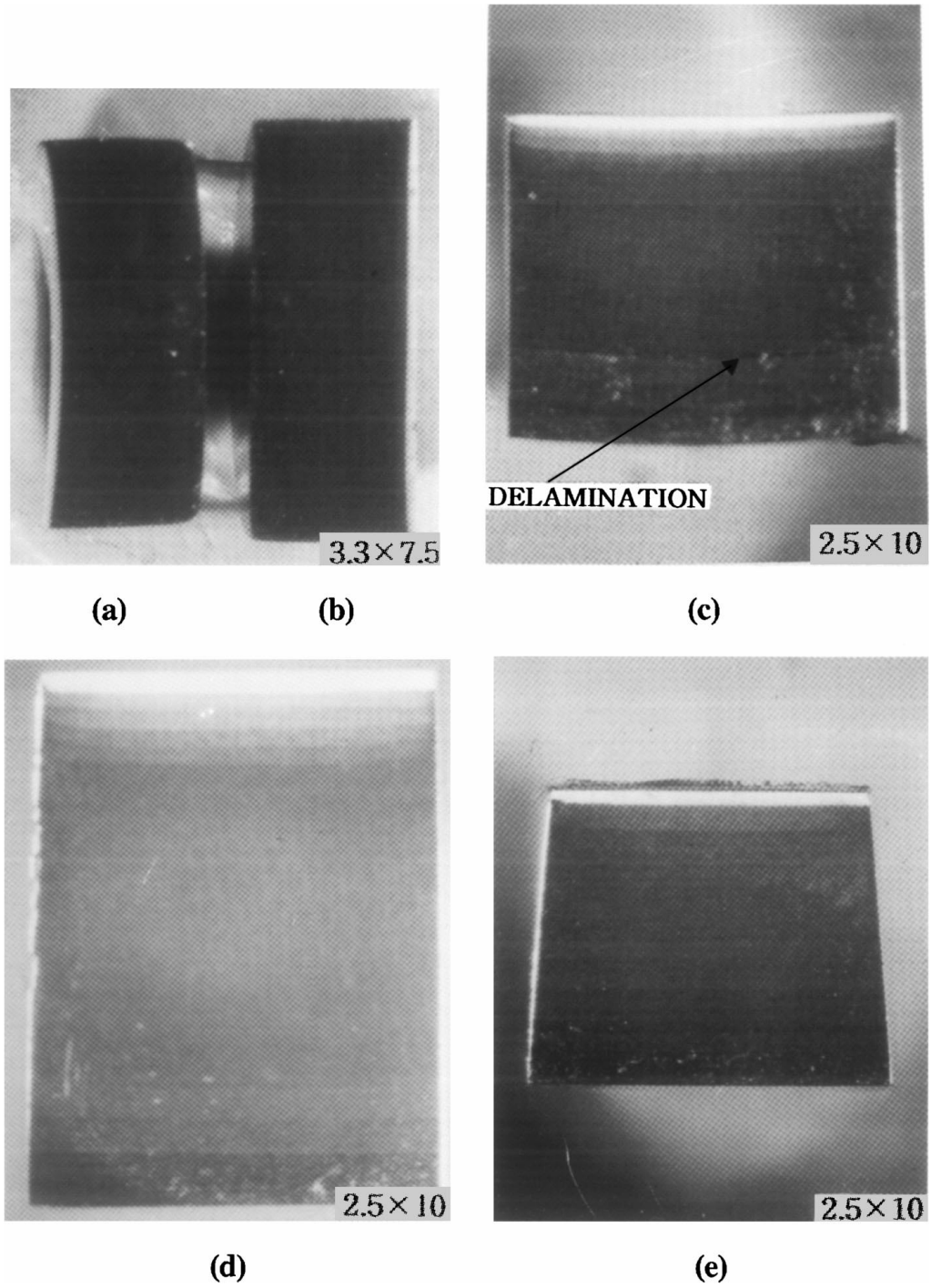

Figure 6 Photographs of sintering samples: (a) TZP/SUS304-FGP having 9 interlayers of thin thickness; (b) ZT/SUS304-FGP having 9 interlayers of thin thickness; (c) TZP/SUS304-FGP having 9 interlayers of thick thickness; (d) TZP/SUS304-FGP having 19 interlayers of thick thickness; and (e) ZT/SUS304-FGP having 9 interlayers of thick thickness.

residual stresses generated on cooling. Consequently, the difference of the shrinkage and sintering behavior and the CTEs of layers can be decreased by the adjustments of the particle size and phase type of starting powders. Therefore, it can be known that, as previously mentioned, the sintering defects are controlled by the decrease of the difference of the sintering shrinkage and CTEs of each layer.

3.2. Residual stress analysis

In the fabrication of FGM or DJM, residual stresses can be induced at the interface or in the inside of materials. During cooling from the fabrication temperature, complex residual stresses are developed, which depend on the inhomogeneous shrinkage and sintering behavior, the difference in the CTEs, the elastic-plastic properties of the components, and the cooling and the joining conditions. These residual stresses induced during the fabrication process play a dominant role in the fracture of materials and make the application under severe environments difficult [11, 26, 27]. Consequently, the residual stress states in such materials and the variation with fabrication conditions are of great importance. Thus, the stress distributions induced on the ceramic regions are examined with the indentation method, and

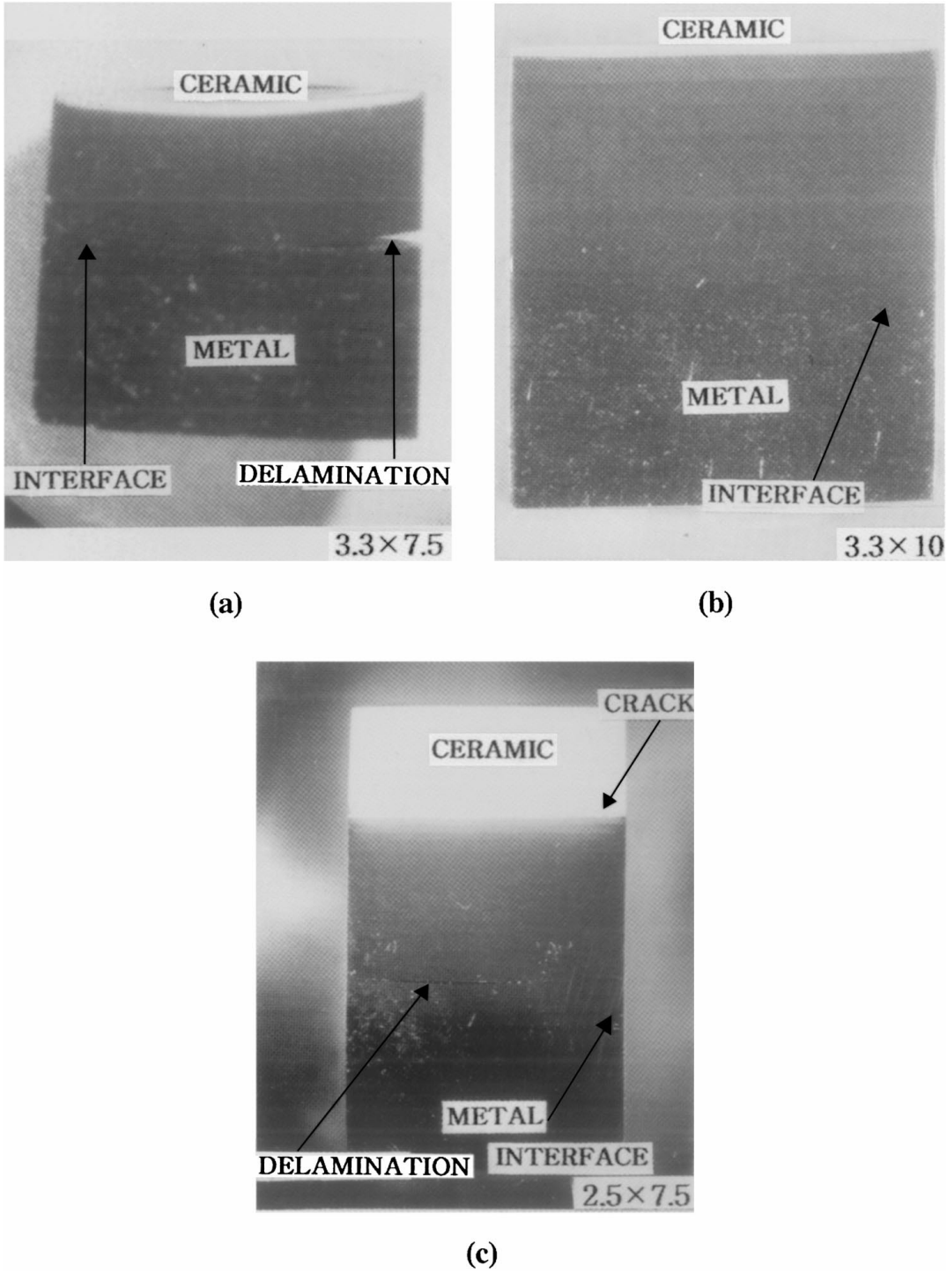

Figure 7 Photographs of sintering samples: (a) TZP/SUS304-FGC having 9 interlayers of thin thickness; (b) ZT/SUS304-FGC having 9 interlayers of thick thickness; and (c) TZP/SUS304-FGJ having 19 interlayers of thin thickness.

the residual stresses generated on the ceramic and metal regions of FGP and FGC are characterized by XRD and compared to stresses in DJM.

As shown in Fig. 9, the cracks propagated from the four corners of the Vickers indent are well-developed with a similar dimension in both the TZP- and ZT-monoliths. However, in TZP/SUS304-FGM and ZT/SUS304-FGM, having 9 interlayers, the length of the crack parallel to the interface is longer than that of the cracks perpendicular to the interface, as shown in Fig. 10. This behavior is direct evidence of compressive stress parallel to the interface and tensile stress perpendicular to the interface. From this result, comparative measurement of crack dimension on the surface in the ceramic-monolith and FGM may reasonably be expected to yield information on residual stress.

X-ray residual stress measurement was performed on the ceramic and metal regions in the parallel direction to the interface. In the case of ZT/SUS304-FGM, the determination of stress states in the ceramic regions is the TZP phase. The measurement positions, as shown in Fig. 11, are interface and surface, and the relative positions of specimen are center and edge. The measured residual stresses are listed in Table III for ceramic and in Table IV for metal. In the TZP/SUS304 joint, the stress states are, on the whole, compressive

TABLE III Residual stress induced on the ceramic regions of each FGM, which is measured by XRD

Position	Residual stress for ZrO_2 (3 3 1) plane	
Specimen	Center	Edge
TZP/SUS304 joint (surface)	-199.04 ± 0.6	-64.29 ± 1.93
TZP/SUS304 joint (interface)	-64.58 ± 5.09	-122.30 ± 1.68
TZP/SUS304-FGP (11 thin layers)	$+200.21 \pm 1.11$	-21.76 ± 3.11
TZP/SUS304-FGP (21 thin layers)	-11.47 ± 0.44	-182.38 ± 4.28
TZP/SUS304-FGC (11 thin layers)	$+154.84 \pm 0.43$	-15.48 ± 3.11
ZT/SUS304 joint (interface)	-132.3 ± 3.81	-216.29 ± 9.42
ZT/SUS304-FGP (11 thin layers)	-757.15 ± 12.51	-400.43 ± 21.05
ZT/SUS304-FGP (11 thick layers)	-274.50 ± 18.09	-142.98 ± 3.50
ZT/SUS304-FGC (11 thick layers)	-995.78 ± 23.57	-533.41 ± 17.39
ZT/SUS304-FGC (11 thick layers)	-243.33 ± 8.68	-27.93 ± 0.75

(−) compressive stress; (+) tensile stress

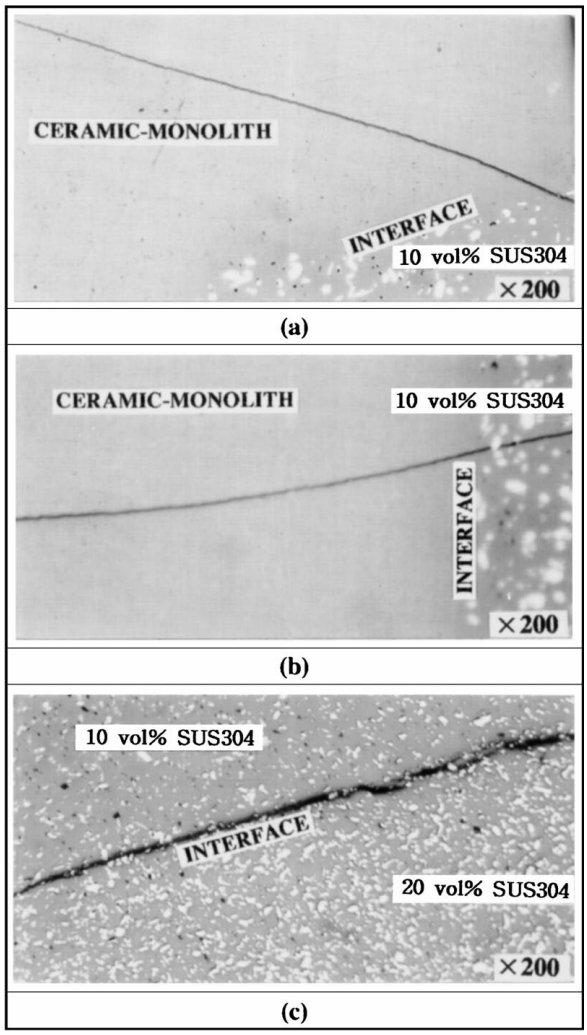

Figure 8 Optical micrographs of crack generated in TZP/SUS304-FGM: (a) TZP/SUS304-FGP (9 interlayers); (b) TZP/SUS304-FGC (9 interlayers); and (c) TZP/SUS304-FGJ (interface between 10 vol % ~ 20 vol % SUS304).

in the ceramic regions, which is the same stress state as shown in Fig. 10. Thus, it can be assumed that tensile stress perpendicular to the interface is induced, and residual stresses change at each position, resulting from the relaxation of stresses by the cracks created in the ceramic regions. Tensile stress is induced on the center of the metal surface, and compressive stress is induced on the others of the metal regions. It is thought that these results are influenced by the sintering defects derived from the shrinkage and sintering behavior of the two components and the different CTEs of ceramic and metal materials. In TZP/SUS304-FGP, the stress states in the ceramic regions change from tensile to compressive, and compressive stress is increased as the number of layers is increased. The opposite stress states, in the case of 11 layers, are developed in the ceramic and metal regions because the stresses induced on the ceramic and metal regions are mutually influenced by the relatively thin interlayer thickness. In the case of 21 layers, compressive stress is increased as the distance is drawn near the edge. In TZP/SUS304-FGC, compressive stresses are induced at the interface and on the surface of the metal, and these stress states are reversed in the center and edge. Tensile stress generated on the center of the ceramic is due to the interaction of the warping to the ceramic direction during sintering and the stress derived from the difference of the CTEs, which may develop warping to the metal direction. As a result, the delamination shown in Fig. 7a is created at the interface of the metal regions. Residual stress developed in TZP/SUS304-FGM, on the whole, does not exhibit an obvious tendency. This indicates, in the case of TZP/SUS304-FGM, that residual stress has already been relaxed by the cracking, warping, and delamination that are created in the ceramic regions and at the interface of the metal and the metal-rich regions.

Generally, in the case of $\alpha_{\text{ceramic}} < \alpha_{\text{metal}}$, tensile stress perpendicular to the interface and compressive stress parallel to the interface are generated on the ceramic surface, while opposite stress states are developed on the metal surface. But TZP/SUS304 and ZT/SUS304 systems with differential shrinkage and sintering behavior do not meet these conditions due to the interaction of defects and residual stress, which result from the shrinkage and sintering behavior and the difference of CTEs, respectively.

Residual stress in ZT/SUS304-FGP is compressive in the ceramic and metal regions. The stress states in the ceramic regions result from the volume expansion of MZP, which induces the compressive stress in TZP and the difference of CTEs ($\alpha_{\text{ceramic}} < \alpha_{\text{metal}}$). Compressive stress on the metal regions is thought to be due to the constrained warping or frustum formation. Compressive stresses on the ceramic and metal regions

TABLE IV Residual stress induced on the metal regions of each FGM, which is measured by XRD

Position	Residual stress for SUS (2 2 0) plane	
Specimen	Center	Edge
TZP/SUS304 joint (surface)	+230.2 ± 14.17	−366.52 ± 9.09
TZP/SUS304 joint (interface)	−294.39 ± 13.47	−233.44 ± 4.37
TZP/SUS304-FGP (11 thin layers)	−261.66 ± 9.73	+257.25 ± 10.77
TZP/SUS304-FGP (21 thin layers)	−88.40 ± 8.37	−264.21 ± 3.94
TZP/SUS304-FGC (11 thin layers, surface)	−84.18 ± 2.08	−174.15 ± 2.01
TZP/SUS304-FGC (11 thin layers, interface)	−303.70 ± 7.69	−46.26 ± 1.16
ZT/SUS304 joint (interface)	−300.76 ± 10.67	−457.76 ± 39.04
ZT/SUS304-FGP (11 thin layers)	−277.26 ± 2.07	−736.47 ± 52.4
ZT/SUS304-FGP (11 thick layers)	−244.51 ± 4.87	−412.38 ± 11.79
ZT/SUS304-FGC (11 thin layers, surface)	−132.52 ± 41.09	−132.68 ± 32.62
ZT/SUS304-FGC (11 thin layers, interface)	−506.07 ± 16.68	−648.66 ± 37.34
ZT/SUS304-FGC (11 thick layers, surface)	−159.05 ± 0.87	−194.43 ± 13.61
ZT/SUS304-FGC (11 thick layers, interface)	−257.74 ± 7.49	−509.49 ± 10.79

(−) compressive stress; (+) tensile stress

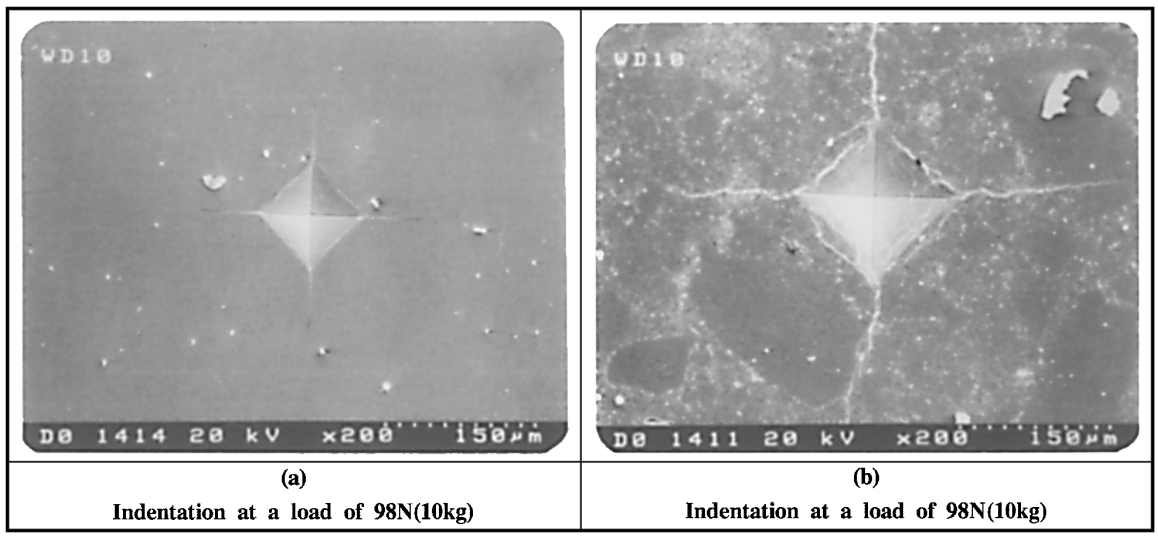

Figure 9 Scanning electron micrographs of the radial cracks developed on TZP- and ZT-monoliths: (a) TZP and (b) ZT.

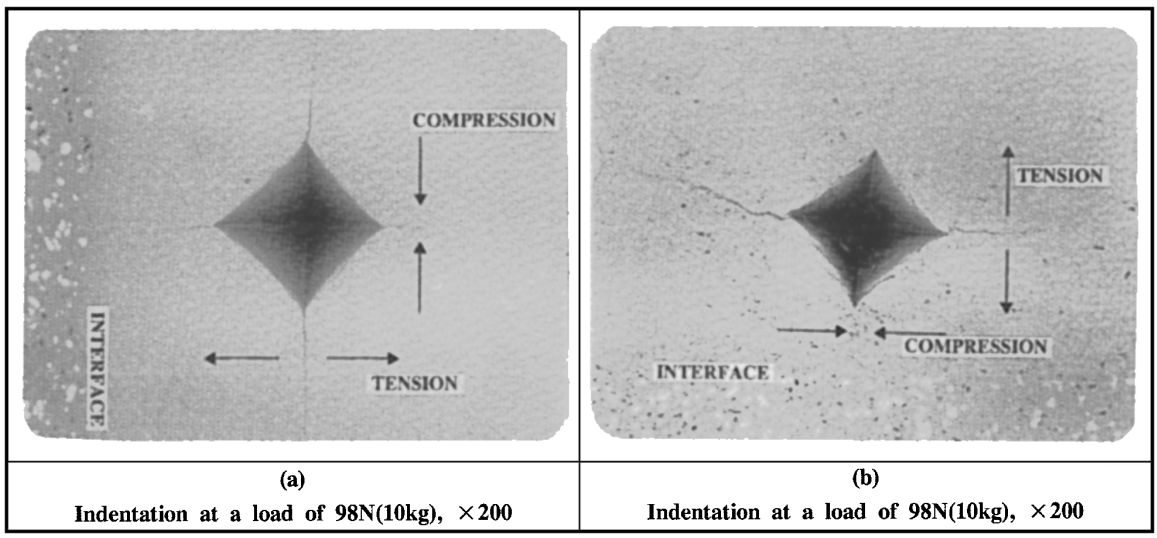

Figure 10 Optical micrographs of the radial cracks developed on the ceramic regions of TZP/SUS304- and ZT/SUS304-FGM: (a) TZP/SUS304-FGM and (b) ZT/SUS304-FGM.

are decreased as the thickness of layer is increased. The stress decreased toward the edge in the ceramic as opposed to the metal, where it increased. The stress states in ZT/SUS304-FGC have the same tendency as those in ZT/SUS304-FGP. The residual stresses developed at the interface of the metal regions are generally greater than that on the surface, and the residual stresses are decreased as the distance from the surface is far away.

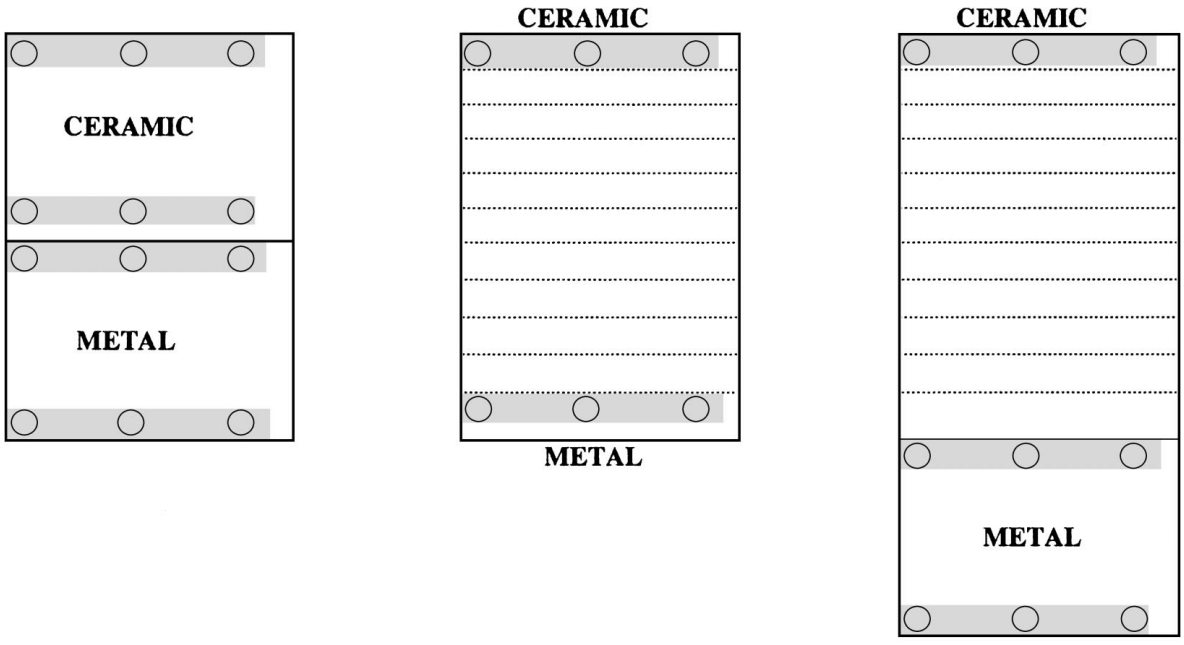

Figure 11 Schematics of the positions in each specimen measured with XRD: (a) directly jointed material; (b) FGP; and (c) FGC.

These results agree qualitatively with the stress distribution determined from indentation examination. It appears that the flaws in the material result in irregular stress patterns. Therefore, fabrication of sound FGM can result from the adjustments of the particle size and phase type of starting powders. In addition, because residual stress is increased with the decrease of the thickness of the interlayer and the flaws are relieved with increasing the number of the interlayer, further development is needed for the fabrication of FGM having a large dimension and a thin interlayer.

4. Conclusions

Various kinds of TZP/SUS304-FGM and ZT/SUS304-FGM were fabricated by pressureless sintering. At this time, the sintering defects owing to differential sintering shrinkage of the starting components could be controlled by the adjustments of the particle size and phase type of zirconia. Flaws in TZP/SUS304-FGM, such as the radial cracks on the ceramic regions, the delamination in the metal-rich regions, and warping, result from the difference of sintering shrinkage and CTEs.

Inhomogeneous residual stresses induced in TZP/SUS304-FGM and -joint result from the defects developed during the fabrication process. The stress states generated on the ceramic and metal regions of ZT/SUS304-FGM are compressive. Compressive stress on the ceramic and metal regions is due to the volume expansion of MZP and the interaction of the sintering behavior and the CTEs, respectively. This compressive stress was also found by indentation crack-length measurements. The magnitude of the stress decreased as the thickness of the layer is increased. In the ceramic regions of ZT/SUS304-FGP and ZT/SUS304-FGC, the residual stress decreased from the center but increased in the metal regions from the center. In the metal regions, residual stress shows a tendency to decrease at the surface rather than at the interface.

The residual stress states generated on FGM are strongly influenced by flaws in the specimen as well as by the thickness and number of compositional gradient layers.

References

1. T. HIRAI, *J. Japan Powder and Powder Metall. Soc.* **37** (1990) 60.
2. M. NIINO, *ibid.* **37** (1990) 61.
3. G. WOLFGANG and J. BUNK, in "Proceedings of the 1st International Symposium on FGM," edited by M. YAMANOUCHI, M. KOIZUMI, T. HIRAI, and I. SHIOTA (Sendai, Japan, October 1990) pp. 1–2.
4. M. NIINO and Y. ISHIBASHI, *J. Japan Comp. Mat. Soc.* **16** (1990) 14.
5. M. KOIZUMI, in "Proceedings of the 1st International Symposium on FGM," edited by M. YAMANOUCHI, M. KOIZUMI, T. HIRAI, and I. SHIOTA (Sendai, Japan, October 1990) pp. 3–4.
6. J. ZHAO, L. C. STEARNS, M. P. HARMER, H. M. CHAN, and G. A. MILLER, *J. Am. Ceram. Soc.* **76** (1993) 503.
7. O. KIMURA and T. KAWASHIMA, *J. Japan Powder and Powder Metall. Soc.* **34** (1987) 1.
8. O. KIMURA, *ibid.* **34** (1987) 518.
9. O. KIMURA and T. KAWASHIMA, *ibid.* **36** (1989) 1.
10. M. KOIZUMI, *Ceram. Eng. Sci. Proc.* **13** (1992) 333.
11. M. SASAKI and T. HIRAI, *The Centennial Memorial Issue of the Ceramic Society of Japan* **99** (1991) 1002.
12. M. NIINO and M. SASAKI, *J. IEE Japan* **110** (1990) 35.
13. M. NIINO and T. KAWAI, *Electronic Mat.* **8** (1991) 103.
14. R. WATANABE, *MRS Bull.*, (1995) pp. 32–34.
15. R. WATANABE and A. KAWASAKI, *J. Japan Powder and Powder Metall. Soc.* **39** (1992) 279.
16. B. EIGENMAN, B. SCHOLTES, and E. MACHERAUCH, *Mat. Sci. Engng.* **A118** (1989) 1.
17. O. T. IANCU, D. MUNZ, B. EIGENMAN, B. SCHOLTES, and E. MACHERAUCH, *J. Am. Ceram. Soc.* **75** (1990) 1144.
18. G. R. ANSTIS, P. CHANTIKUL, B. R. LAWN, and D. B. MARSHALL, *ibid.* **64** (1981) 533.

19. F. F. LANGE, *J. Mat. Sci*. **17** (1982) 225.
20. M. T. HERNANDEZ, J. R. JURADO, and P. DURAN, *J. Am. Ceram. Soc*. **74** (1991) 1254.
21. C. R. BARRETT, W. D. NIX, and A. S. TETELMAN, *Metall. Trans*. **14A** (1983) 1907.
22. E. MACHERAUCH and P. MÜLLER, *Z. Angew. Phys.* **13** (1961) 305.
23. R. WATANABE et al., "Functionally Gradient Materials" (Kogyo Chosakai Publishing Co. Ltd., 1993) pp. 36–57.
24. R. WATANABE and A. KAWASAKI, in "Proceedings of the 1st International Symposium on FGM," edited by M. YAMANOUCHI, M. KOIZUMI, T. HIRAI, and I. SHIOTA (Sendai, Japan, October 1990) pp. 107–113.
25. M. L. SANTELLA, *Ceram. Bull*. **71** (1992) 947.
26. Y. ITOH and H. KASHIWAYA, *J. Japan Ceram. Soc.* **100** (1992) 476.

Received 2 January 1997
and accepted 17 August 1998